International Journal of Heat and Mass Transfer 52 (2009) 2092–2101

Contents lists available at ScienceDirect

International Journal of Heat and Mass Transfer

journal homepage: www.elsevier.com/locate/ijhmt

Temperature field in a moving semi-infinite region with a prescribed wall heat flux

A. Haji-Sheikh [a,*], Donald E. Amos [b], J.V. Beck [c]

[a] Department of Mechanical and Aerospace Engineering, The University of Texas at Arlington, 500 W First Street, Arlington, TX 76019-0023, USA
[b] Sandia National Laboratories, Albuquerque, NM 87110, USA
[c] Department of Mechanical Engineering, Michigan State University, East Lansing, MI 48824-1226, USA

ARTICLE INFO

Article history:
Received 29 September 2008
Received in revised form 5 November 2008
Available online 26 December 2008

Keywords:
Heat transfer
Moving boundary
Axial conduction
Slug flow
Thermal entrance

ABSTRACT

Steady state conduction of heat from a stationary wall to a medium moving at a uniform velocity is the subject herein. This medium can be a solid or a fluid moving at a constant velocity. The surface of this medium is insulated until a change in the surface heat flux occurs. The determination of temperature field is the main objective herein. The results show that the surface temperature begins to increase before its arrival to the heater's location where there is an abrupt change in the surface heat flux. The application of this phenomenon to a moving wall with frictional heating at its surface and to classical heat transfer in ducts can lead to new information.

1. Introduction

Analytical studies of convective heat transfer in the presence of axial conduction within fluid passages are reported by many investigators. A study for flow between parallel plates at small Peclet numbers is in Agrawal [1]. The Graetz-type solution is also extended to include the effect of axial conduction by other investigators, e.g., Henneck [2] and Bayazitoglu and Ozisik [3]. Other related heat transfer studies in the presences of axial conduction are in [4–12]. Also, the effect of axial conduction can evolve during heat transfer through microchannels [13]. These and other similar studies use series solutions that converge slowly where there is a step change in the wall condition. For slug flow, a closed-form exact solution of heat transfer from the wall to a moving semi-infinite domain with a step change in the wall temperature is in [14]. It provides the limiting solution for heat transfer coefficient at very small distance from the location of temperature changes in other flow passages [15,16]. The present work is a continuation of the mathematical formulation in [14] modified for the boundary condition of the second kind at the wall. As reported in [14–16], the thermal conduction dominates near the wall at small distances from the location where the wall temperature changes. This phenomenon, when there is a step change in the wall heat flux, provides related but different information for the determination of wall temperature and temperature field in various-shaped ducts.

The case of slug flow presented here has direct applications to flow in porous passages. In these passages, permeability controls the effective thermal conductivity and the Darcy number [17–20]. Therefore, the slug flow becomes a reasonable limiting case when the Darcy number is very small. Additionally, when the fluid velocity in a packed porous passage is small, the Peclet number can become small. For an alternative application, one can view this moving medium as a solid moving over a contact zone with another solid. The heat generated due to frictional heating is the wall heat flux that depends on the applied pressure.

The first mathematical formulation given herein and subsequent numerical calculations include the effect of axial conduction of heat in the flow direction parallel to a wall, as shown in Fig. 1. Fig. 1 shows a semi-infinite medium is moving with uniform velocity over a thermally insulated stationary infinite wall when $\hat{x} < 0$ and there is a prescribed finite wall heat flux q_w when $\hat{x} > 0$. Furthermore, the medium with an approaching temperature T_i occupies a region between $\hat{y} = 0$ and $\hat{y} = \infty$. This condition also corresponds to the slug flow approximation for the study of heat transfer in fluid saturated porous passages. Therefore, it can provide limiting values for the wall temperature and the corresponding heat transfer coefficient when the permeability is very small. The methodology presented in this study leads to a closed-form solution that provides accurate information as $\hat{x}$ goes toward zero. The numerical results directly apply to heat transfer to slug flow in fluid saturated porous passages when the temperature penetration at the entrance location is small. Also, as expected, this solution provides an upper limit for the values of the Stanton number.

* Corresponding author. Tel.: +1 817 272 2010; fax: +1 817 272 5010.
E-mail address: haji@uta.edu (A. Haji-Sheikh).

0017-9310/$ - see front matter © 2008 Elsevier Ltd. All rights reserved.
doi:10.1016/j.ijheatmasstransfer.2008.11.005

Nomenclature

A_m,B_m	constants in series solutions
c_p	specific heat, J/kg K
D_h	hydraulic diameter, m
$g(x)$	Boundary condition in Eq. (3), K
h	$q_w/(T_w - T_b)$, W/m^2 K
h_0	$q_w/(T_w - T_i)$, W/m^2 K
H	half distance between plates, m
k	thermal conductivity, W/m K
L_c	stands for W, H, or r_0, m
$\mathrm{Nu_D}$	hD_h/k
Pe	Peclet number UL_c/α
$q(x,y)$	heat flux function, W/m^2
q_w	wall heat flux when $x > 0$, W/m^2
$\hat{r}$	radial coordinate, m
r	$\hat{r}/r_0$
r_0	pipe radius, m
St	Stanton number $h/(\rho c_p U)$
T	temperature, K
T_i	temperature when $\hat{x} \to -\infty$, K
U	velocity, m/s
W	fluid layer thickness, m
x	$\hat{x}/L_c$
$\hat{x}$	axial coordinate, m
y	$\hat{y}/L_c$
$\hat{y}, \hat{z}$	coordinates, m

Greek symbols

α	thermal diffusivity, m^2/s
β_m	axial eigenvalue when $x < 0$
γ_m	eigenvalue
ε	a constant, 0 or 1
η	parameter for y or r
θ	reduced temperature $T(x,y) - T_i$, K
λ	dummy variable
λ_m	axial eigenvalue when $x > 0$
ξ	dummy variable
ρ	density, kg/m^3
Φ	reduced dimensionless temperature
Ψ	special eigenfunction
ω	$UW/2\alpha$

Subscripts

1	when $\hat{x} < 0$
2	when $\hat{x} > 0$
b	bulk temperature
w	wall

2. Mathematical formulation for semi-infinite domains

As stated earlier, the domain of interest is a semi-infinite region when $-\infty < x < +\infty$ and $0 \leqslant y < +\infty$. The steady state energy equation assuming constant thermophysical properties is

$$k\left(\frac{\partial^2 T}{\partial \hat{x}^2} + \frac{\partial^2 T}{\partial \hat{y}^2}\right) = \rho c_p U \frac{\partial T}{\partial \hat{x}} \tag{1}$$

where U is a uniform velocity while k, ρ, and c_p are the fluid's thermal conductivity, density, and specific heat. Using a reduced temperature defined as $\theta = T - T_i$ and dimensionless quantities $x = \hat{x}/W$, $y = \hat{y}/W$, and $\omega = UW/2\alpha$, Eq. (1) takes the form

$$\frac{\partial^2 \theta}{\partial x^2} + \frac{\partial^2 \theta}{\partial y^2} = 2\omega \frac{\partial \theta}{\partial x} \tag{2}$$

where $\alpha = k/(\rho c_p)$. The parameter W is an arbitrarily selected length and it can be the width of a fluid layer in the $\hat{z}$ direction perpendicular to $\hat{x}\hat{y}$-plane, depicted in Fig. 1. The main task is determination of a solution for Eq. (2) that satisfies the boundary conditions

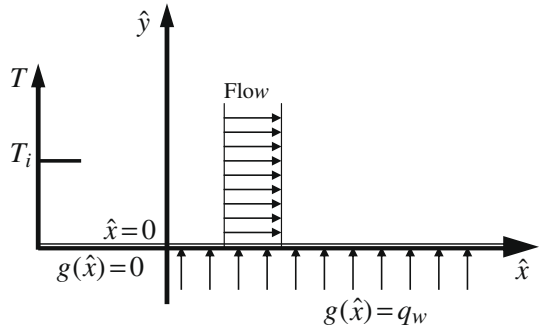

Fig. 1. Schematic of a moving body with a finite wall heat flux when $\hat{x} \geqslant 0$.

$$\begin{cases} \theta(x,\infty) = 0 \\ \partial\theta/\partial y = -g(x) \text{ when } y = 0 \\ \theta(-\infty, y) = 0 \\ \partial\theta/\partial y = \text{finite as } x \to \infty \end{cases} \tag{3}$$

The mathematical procedure begins by using the transformation

$$\theta(x,y) = e^{\omega x}\psi(x,y) \tag{4}$$

to have Eq. (2) taking the form

$$\frac{\partial^2 \psi}{\partial x^2} + \frac{\partial^2 \psi}{\partial y^2} - \omega^2 \psi = 0. \tag{5}$$

As described in [14], the solution of this equation is obtainable by letting $\psi = X(x)Y(y)$ in order to separate the variables and to get

$$\frac{X''}{X} = -\frac{Y''}{Y} + \omega^2 = -\lambda^2 \tag{6}$$

with λ is being a constant. The solutions for functions X and Y are $X = \exp(\pm i\lambda x)$ and $Y = \exp(-y\sqrt{\lambda^2 + \omega^2})$, since y varies between 0 and $+\infty$. This leads to a classical integral transform as given in [21] and in [22, Section 17.21, P. 1183]

$$\psi(x,y) = \int_{-\infty}^{+\infty} A(\lambda)\exp(i\lambda x)\exp\left(-y\sqrt{\lambda^2 + \omega^2}\right)d\lambda. \tag{7}$$

Then, the reduced temperature solution, using Eq. (4), becomes

$$\theta(x,y) = e^{\omega x}\int_{-\infty}^{+\infty} A(\lambda)\exp(i\lambda x)\exp\left(-y\sqrt{\lambda^2 + \omega^2}\right)d\lambda. \tag{8}$$

Applying, the prescribed wall heat flux condition $\partial\theta/\partial y = -g(x)$ when $y = 0$, leads to a Fourier integral [21,22]

$$\begin{aligned} g(x) &= e^{\omega x}\int_{-\infty}^{+\infty} A(\lambda)\exp(i\lambda x)\sqrt{\lambda^2 + \omega^2}\,d\lambda \\ &= \int_{-\infty}^{+\infty} B(\lambda)\exp(i\lambda x)d\lambda \end{aligned} \tag{9}$$

for determination of

$$B(\lambda)=\frac{1}{2\pi}\int_{-\infty}^{+\infty}[\exp(-\omega\xi)g(\xi)]\exp(-i\lambda\xi)d\xi \tag{10}$$

where $B(\lambda)=A(\lambda)\sqrt{\lambda^2+\omega^2}$ in Eq. (9). Then, the coefficient $A(\lambda)$ becomes

$$A(\lambda)=\frac{1}{2\pi\sqrt{\lambda^2+\omega^2}}\int_{-\infty}^{+\infty}[\exp(-\omega\xi)g(\xi)]\exp(-i\lambda\xi)d\xi. \tag{11}$$

Now, for the special case under consideration, the dimensional heat flux function $g(x)$ is defined as

$$g(x)=\begin{cases}0 \text{ when } x<0\\ q_wW/k \text{ when } x>0\end{cases}. \tag{12}$$

After substitution for $g(x)$ in Eq. (11), it becomes

$$\begin{aligned}A(\lambda)&=\frac{q_wW/k}{2\pi\sqrt{\lambda^2+\omega^2}}\int_0^{+\infty}\exp\left[-(\omega+i\lambda)\xi\right]d\xi\\&=\frac{1}{2\pi}\left(\frac{1}{\omega+i\lambda}\right)\left(\frac{q_wW/k}{\sqrt{\lambda^2+\omega^2}}\right)\end{aligned} \tag{13}$$

and then the substitution for $A(\lambda)$ in Eq. (8) provides the following relation

$$\frac{\theta(x,y)}{q_wW/k}=\frac{e^{\omega x}}{2\pi}\left[\int_{-\infty}^{0}\frac{e^{i\lambda x}e^{-y\sqrt{\lambda^2+\omega^2}}}{(\omega+i\lambda)\sqrt{\lambda^2+\omega^2}}d\lambda+\int_0^{\infty}\frac{e^{i\lambda x}e^{-y\sqrt{\lambda^2+\omega^2}}}{(\omega+i\lambda)\sqrt{\lambda^2+\omega^2}}d\lambda\right]. \tag{14}$$

The wall temperature at $y=0$ is an important parameter for determination of the heat transfer coefficient

$$\frac{\theta(x,0)}{q_wW/k}=\frac{e^{\omega x}}{2\pi}\left[\int_{-\infty}^{0}\frac{e^{i\lambda x}}{(\omega+i\lambda)\sqrt{\lambda^2+\omega^2}}d\lambda+\int_0^{\infty}\frac{e^{i\lambda x}}{(\omega+i\lambda)\sqrt{\lambda^2+\omega^2}}d\lambda\right]. \tag{15}$$

The last two equations are valid for positive and negative x values. They have real and imaginary components which can be determined. This task can be accomplished by multiplying the numerators and the denominators by $\omega-i\lambda$, replacing $\exp(i\lambda x)$ by $\cos(\lambda x)+i\sin(\lambda x)$, and following standard algebraic steps to get

$$\begin{aligned}\frac{e^{i\lambda x}}{(\omega+i\lambda)}&=\frac{\cos(\lambda x)+i\sin(\lambda x)}{(\omega+i\lambda)}\frac{(\omega-i\lambda)}{(\omega-i\lambda)}\\&=\frac{\omega\cos(\lambda x)+\lambda\sin(\lambda x)}{(\omega^2+\lambda^2)}+i\frac{\omega\sin(\lambda x)-\lambda\cos(\lambda x)}{(\omega^2+\lambda^2)}.\end{aligned} \tag{16}$$

Since the real part of $\theta(x{\cdot}y)$ is the solution in Eq. (14), only the real part of Eq. (16) is to be retained. Then, the real parts of the complex integrals in Eq. (14) would become the temperature solution. Accordingly, after inserting the real part of Eq. (16) into Eq. (14), the temperature solution takes the form

$$\frac{\theta(x,y)}{q_wW/k}=\frac{e^{\omega x}}{\pi}\left[\int_0^{\infty}\frac{e^{-y\sqrt{\lambda^2+\omega^2}}\omega\cos(\lambda x)}{(\lambda^2+\omega^2)^{3/2}}d\lambda+\int_0^{\infty}\frac{e^{-y\sqrt{\lambda^2+\omega^2}}\lambda\sin(\lambda x)}{(\lambda^2+\omega^2)^{3/2}}d\lambda\right]. \tag{17}$$

It is possible to produce an integrated form of Eq. (17) for determination of the temperature as a function of x at $y=0$ location. To accomplish this task, one can use [Eq. (3.962) in 21] to get these two integrals related to the modified Bessel functions

$$\int_0^{+\infty}e^{-y\sqrt{\lambda^2+\omega^2}}\frac{\lambda\sin(\lambda x)}{\sqrt{\lambda^2+\omega^2}}d\lambda=\frac{\omega x}{\sqrt{x^2+y^2}}K_1\left[\omega\sqrt{x^2+y^2}\right] \tag{18a}$$

and

$$\int_0^{+\infty}e^{-y\sqrt{\lambda^2+\omega^2}}\frac{\cos(\lambda x)}{\sqrt{\lambda^2+\omega^2}}d\lambda=K_0\left[\omega\sqrt{x^2+y^2}\right]. \tag{18b}$$

The integrals in Eq. (17) are obtainable by differentiating both sides of Eqs. (18a,b) with respect to ω to get

$$\begin{aligned}&\int_0^{+\infty}e^{-y\sqrt{\lambda^2+\omega^2}}\frac{\lambda\sin(\lambda x)}{(\lambda^2+\omega^2)^{3/2}}d\lambda\\&=-\int_0^{+\infty}ye^{-y\sqrt{\lambda^2+\omega^2}}\frac{\lambda\sin(\lambda x)}{\lambda^2+\omega^2}d\lambda\\&\quad-\frac{x}{\omega\sqrt{x^2+y^2}}K_1\left[\omega\sqrt{x^2+y^2}\right]\\&\quad+\frac{x}{2}\left[K_0\left(\omega\sqrt{x^2+y^2}\right)+K_2\left(\omega\sqrt{x^2+y^2}\right)\right]\end{aligned} \tag{19a}$$

and

$$\begin{aligned}&\int_0^{+\infty}e^{-y\sqrt{\lambda^2+\omega^2}}\frac{\cos(\lambda x)}{(\lambda^2+\omega^2)^{3/2}}d\lambda\\&=-\int_0^{+\infty}ye^{-y\sqrt{\lambda^2+\omega^2}}\frac{\cos(\lambda x)}{\lambda^2+\omega^2}d\lambda\\&\quad+\frac{\sqrt{x^2+y^2}}{\omega}K_1\left(\omega\sqrt{x^2+y^2}\right).\end{aligned} \tag{19b}$$

The left side of Eq. (19a) and the left side of Eq. (19b) are the two integrals within Eq. (17) and, after substitution, Eq. (17) becomes

$$\begin{aligned}\frac{\theta(x,y)}{q_wW/k}=\frac{e^{\omega x}}{\pi}\Bigg\{&-\frac{x}{\omega\sqrt{x^2+y^2}}K_1\left(\omega\sqrt{x^2+y^2}\right)+\frac{x}{2}\Big[K_0\left(\omega\sqrt{x^2+y^2}\right)\\&+K_2\left(\omega\sqrt{x^2+y^2}\right)\Big]+\sqrt{x^2+y^2}K_1\left(\omega\sqrt{x^2+y^2}\right)\Bigg\}-yF(x,y,\omega)\end{aligned} \tag{20a}$$

wherein

$$F(x,y,\omega)=\frac{e^{\omega x}}{\pi}\left[\int_0^{+\infty}e^{-y\sqrt{\lambda^2+\omega^2}}\frac{\omega\cos(\lambda x)}{\lambda^2+\omega^2}d\lambda+\int_0^{+\infty}e^{-y\sqrt{\lambda^2+\omega^2}}\frac{\lambda\sin(\lambda x)}{\lambda^2+\omega^2}d\lambda\right]. \tag{20b}$$

It is remarkable that this $F(x,y,\omega)$ is also the solution for temperature field in [14] when there is a jump in the wall temperature at $x=0$ location. Then, the values of this function for $x<0$ and $x>0$ domains are

$$F(x,y,\omega)=-\frac{e^{-\omega|x|}}{\pi}\left[\omega\int_0^y K_0\left(\omega\sqrt{x^2+\eta^2}\right)d\eta-\omega|x|\int_0^y\frac{K_1\left(\omega\sqrt{x^2+\eta^2}\right)}{\sqrt{x^2+\eta^2}}d\eta\right] \tag{21a}$$

when $x<0$ and

$$F(x,y,\omega)=1-\frac{e^{\omega x}}{\pi}\left[\omega\int_0^y K_0\left(\omega\sqrt{x^2+\eta^2}\right)d\eta-\omega x\int_0^y\frac{K_1\left(\omega\sqrt{x^2+\eta^2}\right)}{\sqrt{x^2+\eta^2}}d\eta\right] \tag{21b}$$

when $x>0$. Finally, the wall temperature is obtainable from Eq. (20a) when $y=0$; it becomes

$$\frac{2\omega\theta(x,0)}{q_wW/k}=\frac{e^{-\omega|x|}}{\pi}\left[2(\omega|x|+1)K_1(\omega|x|)-\omega|x|K_0(\omega|x|)-\omega|x|K_2(\omega|x|)\right] \tag{22a}$$

when $x<0$ and

$$\frac{2\omega\theta(x,0)}{q_wW/k}=\frac{e^{\omega x}}{\pi}\left[2(\omega x-1)K_1(\omega x)+\omega xK_0(\omega x)+\omega xK_2(\omega x)\right] \tag{22b}$$

when $x>0$. These solutions are the sought integrated forms of Eq. (17) at $y=0$ and Fig. 2 shows the variation of

$$\frac{2\omega\theta(x,0)}{q_wW/k}=\frac{\rho c_pU\theta(x,0)}{q_w} \tag{23}$$

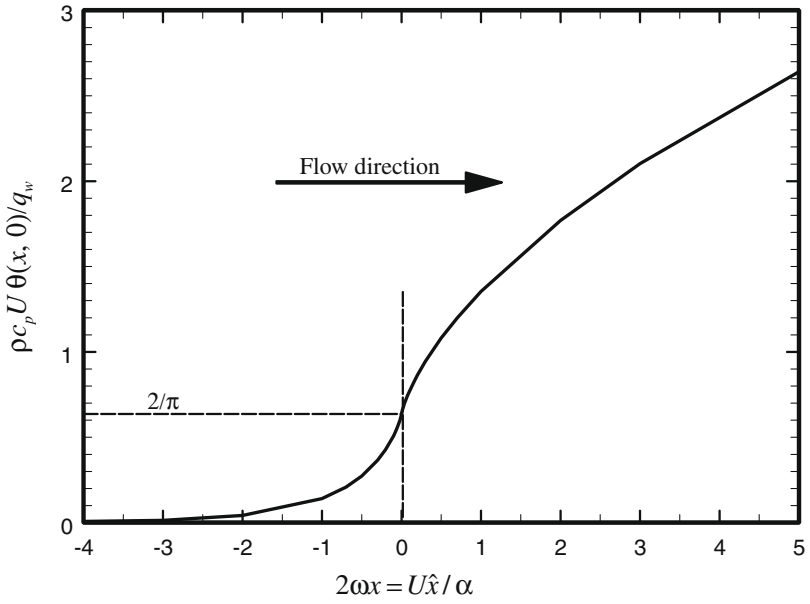

Fig. 2. Dimensionless wall temperature for a semi-infinite moving medium with a step change in surface heat flux as a function of $2\omega x = U\hat{x}/\alpha$.

as a function of $2\omega x = U\hat{x}/\alpha$. When $x < 0$, this dimensionless wall temperature, as defined by Eq. (23), rapidly decreases as $|x|$ increases. However, when $x > 0$, it shows a gradual increase as x increases. The asymptotic values of these modified Bessel functions as x goes toward zero are from Eq. (9.6.13) in [23]

$$K_0(z) \cong -[\ln(z/2) + 0.5772](1 + z^2/2) \tag{24a}$$

and from Eq. (9.6.11) in [23]

$$K_1(z) \cong \frac{1}{z} + \frac{z}{2}\ln(z/2) \tag{24b}$$

with an error less than ±0.5% for $0 < z < 0.45$ while $K_2(z) = K_0(z) + 2K_1(z)/z$.

Once the temperature distribution is known, it is possible to compute the heat transfer coefficient. Defining the heat transfer coefficient as $h_0(x) = q(x,0)/[T(x,0) - T_i]$, it becomes $h_0 = 0$ when $x \geqslant 0$, since $q(x,0) = 0$. However, when $x \geqslant 0$, $q(x,0) = q_w$ is finite and the heat transfer coefficient is $h_0(x) = q(x,0)/[T(x,0) - T_i] = q_w/\theta(x,0)$. According to this definition, the left side of Eq. (22b) takes the form

$$\frac{2\omega\theta(x,0)}{q_w W/k} = \left(\frac{UW}{\alpha}\right)\left(\frac{k}{h_0(x)W}\right) = \frac{\rho c_p U}{h_0(x)} = \frac{1}{\mathrm{St}(x)} \tag{25a}$$

and then, for application to slug flow, the Stanton number St becomes

$$\mathrm{St}(x) = \frac{\pi e^{-\omega x}}{2(\omega x - 1)K_1(\omega x) + \omega x K_0(\omega x) + \omega x K_2(\omega x)}. \tag{25b}$$

Note that the Stanton number is solely a function of the dimensionless parameter $\omega x = U\hat{x}/(2\alpha)$. It is possible to determine the value of the Stanton number at $x = 0$ by placing the asymptotic values of $K_0(\omega x) \sim -\ln(\omega x)$, $K_1(\omega x) \sim 1/(\omega x)$, and $K_2(\omega x) \sim 2/(\omega x)^2$ from [23] in Eq. (25b) to get $\mathrm{St}(0) = \pi/2$. Fig. 3 shows the computed Stanton number $\mathrm{St}(x)$ as a function of $2\omega x = U\hat{x}/\alpha$. Indeed, when $x < 0$, the heat transfer coefficient has a zero value since the wall is insulated and $\theta(x,0)$ has a finite value, as depicted in Fig. 2. However, when $x > 0$, the Stanton number is equal to $2/\pi$ at $x = 0$ and it gradually decreases as x increases.

The temperature distribution when $x = 0$ yields valuable information. When $x = 0$ and y is finite, Eq. (20a) reduces to

$$\frac{2\omega\theta(0,y)}{q_w W/k} = \frac{2\omega y}{\pi}[K_1(\omega y)] - \omega y\left\{\frac{1}{2} - \frac{\omega y}{2}[K_0(\omega y)L_{-1}(\omega y) + K_1(\omega y)L_0(\omega y)]\right\}. \tag{26a}$$

Substituting for $\omega = UW/2\alpha$ reduces this equation to

$$\frac{\theta(0,y)}{q_w/(\rho c_p U)} = \frac{2}{\pi}\left(\frac{Uy}{2\alpha}\right)\left[K_1\left(\frac{Uy}{2\alpha}\right)\right] - \left(\frac{Uy}{2\alpha}\right)\left\{1 - 2\left(\frac{Uy}{2\alpha}\right)\left[K_0\left(\frac{Uy}{2\alpha}\right)L_{-1}\left(\frac{Uy}{2\alpha}\right) + K_1\left(\frac{Uy}{2\alpha}\right)L_0\left(\frac{Uy}{2\alpha}\right)\right]\right\} \tag{26b}$$

where $L_{-1}(Uy/2\alpha)$ and $L_0(Uy/2\alpha)$ are the Struve L-functions [23], Eq. (12.2.1)]. Table 1 shows the values of the dimensionless temperature on the left side of Eq. (26b) as a function of Uy/α at $x = 0$ location. For slug flow through finite passages, this equation applies when the temperature penetration is small. As an example, for a flow between two parallel plated $2H$ apart, the centerline is located at $y = H$. According to the fourth column in Table 1 there is a small temperature penetration toward the centerline near the $x = 0$ location when $UH/\alpha \gtrsim 5$. This concept is further demonstrated in the next section.

3. Heat transfer to flow in other passages

The study of heat transfer in two other geometries, as depicted in Fig. 4, is appearing within this section. One is a moving slab between two stationary walls or it can be viewed as a slug flow between two parallel plates. This geometry is selected for the purpose of verification of the results presented in the earlier section. Then, this analysis is extended to include a circular geometry. In the absence of frictional heating, the energy equation

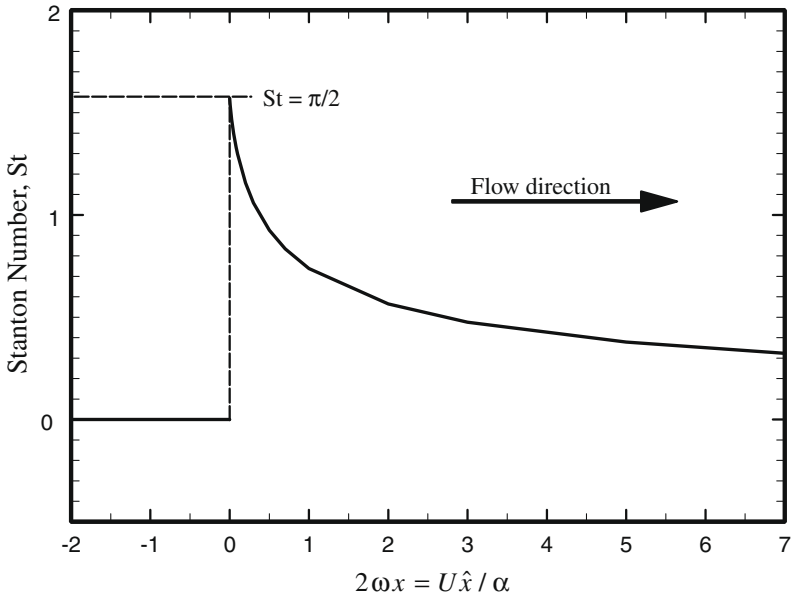

Fig. 3. The Stanton number $h_0(x)/(\rho c_p U)$ for a semi-infinite moving medium with a step change in surface heat flux as a function of $2\omega x = U\hat{x}/\alpha$.

Table 1
Temperature variation in a semi-infinite region at $x = 0$ location as a function of Uy/α.

Uy/α	$\frac{\theta(0,Uy/\alpha)}{q_w/(\rho c_p U)}$	Uy/α	$\frac{\theta(0,Uy/\alpha)}{q_w/(\rho c_p U)}$
0.0	0.63662	5.5	0.02345
0.5	0.446507	6.0	0.017777
1.0	0.322367	6.5	0.013497
1.5	0.235934	7.0	0.010261
2.0	0.174192	7.5	0.00781
2.5	0.129418	8.0	0.00595
3.0	0.096614	8.5	0.004538
3.5	0.072401	9.0	0.003464
4.0	0.054425	9.5	0.002647
4.5	0.04102	10.0	0.002023
5.0	0.030985	∞	0.0

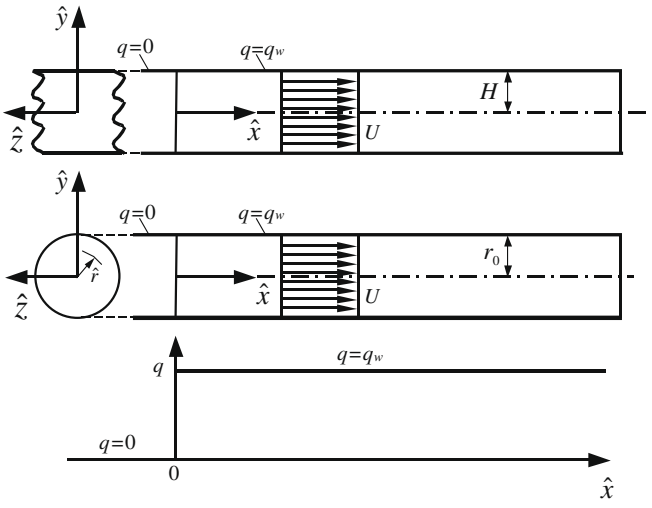

Fig. 4. Schematics and coordinates of a moving flat plate and a moving circular medium.

$$k\left[\frac{\partial^2 T}{\partial \hat{x}^2}+\frac{1}{\hat{\eta}^{\varepsilon}}\frac{\partial}{\partial \hat{\eta}}\left(\hat{\eta}^{\varepsilon}\frac{\partial T}{\partial \hat{\eta}}\right)\right]=\rho c_p U\frac{\partial T}{\partial \hat{x}} \tag{27}$$

is valid subject to the boundary conditions

$$(\partial T/\partial \hat{\eta})_{\hat{\eta}=0}=0 \tag{28a}$$

$$(\partial T/\partial \hat{\eta})_{\hat{\eta}=L_c}=\begin{cases}0 \text{ when } \hat{x}<0\\ q_w/k \text{ when } \hat{x}\geqslant 0\end{cases} \tag{28b}$$

$$T=T_i \text{ as } \hat{x}\to-\infty \tag{28c}$$

$$\frac{\partial T}{\partial \hat{x}}\cong(\varepsilon+1)q_w/(\rho c_p U L_c) \text{ as } (\hat{x}\to+\infty) \tag{28d}$$

where q_w is the wall heat flux (per unit area) entering this fluid passage between $\hat{x}=0$ and ∞. For a moving medium between two parallel plates $2H$ apart, as shown in Fig. 4, $\varepsilon = 0$, $L_c = H$ and $\hat{\eta}$ stands for $\hat{y}$ while for a moving circular medium, shown in Fig. 4, with radius r_0, $\varepsilon = 1$, $L_c = r_0$, and $\hat{\eta}$ stands for radius $\hat{r}$. By defining the dimensionless coordinates as $x=\hat{x}/L_c$, $\eta=\hat{\eta}/L_c$, and $\bar{x}=x/\mathrm{Pe}$, the energy equation as given by Eq. (27) becomes

$$\frac{1}{\eta^{\varepsilon}}\frac{\partial}{\partial \eta}\left(\eta^{\varepsilon}\frac{\partial T}{\partial \hat{\eta}}\right)=\frac{\partial T}{\partial \bar{x}}-\frac{1}{\mathrm{Pe}^2}\frac{\partial^2 T}{\partial \bar{x}^2} \tag{29}$$

where $\mathrm{Pe} = UL_c/\alpha$. The exact temperature solution from Eq. (29) is deterministic if one defines a function $\Phi_1(\bar{x},\eta)$ so that

$$T-T_i=\left(\frac{q_w L_c}{k}\right)\Phi_1(\bar{x},\eta) \tag{30a}$$

when $\bar{x}<0$ and a function $\Phi_2(\bar{x},\eta)$ so that

$$T-T_i=\left(\frac{q_w L_c}{k}\right)\left[\Phi_2(\bar{x},\eta)+(\varepsilon+1)\bar{x}+\frac{1}{2}\eta^2\right] \tag{30b}$$

when $\bar{x}>0$. Substituting these reduced dimensionless temperature functions in Eq. (29), the energy equation takes the following forms

$$\frac{1}{\eta^{\varepsilon}}\frac{\partial}{\partial \eta}\left(\eta^{\varepsilon}\frac{\partial \Phi_1}{\partial \hat{\eta}}\right)=\frac{\partial \Phi_1}{\partial \bar{x}}-\frac{1}{\mathrm{Pe}^2}\frac{\partial^2 \Phi_1}{\partial \bar{x}^2}$$
$$\text{with}\quad \frac{\partial \Phi_1}{\partial \eta}=0 \quad \text{at } \eta=0 \quad \text{and} \quad \text{at } \eta=1 \tag{31a}$$

The functional form of Eq. (30b) is selected so that $\Phi_2(\bar{x},y)$ function satisfies a similar partial differential equation; that is

$$\frac{1}{\eta^{\varepsilon}}\frac{\partial}{\partial \eta}\left(\eta^{\varepsilon}\frac{\partial \Phi_2}{\partial \hat{\eta}}\right)=\frac{\partial \Phi_2}{\partial \bar{x}}-\frac{1}{\mathrm{Pe}^2}\frac{\partial^2 \Phi_2}{\partial \bar{x}^2}$$
$$\text{with}\frac{\partial \Phi_2}{\partial \eta}=0 \quad \text{at } \eta=0 \quad \text{and} \quad \text{at } \eta=1 \tag{31b}$$

The Eqs. (31a,b) represent two classical conduction problems, whose solutions for $\Phi_1(\bar{x},y)$ and $\Phi_2(\bar{x},y)$ functions have the forms

$$\Phi_1(\bar{x},\eta)=\sum_{m=0}^{\infty}A_m\Psi_m(\eta)e^{\beta_m\bar{x}} \text{ when } \bar{x}<0 \tag{32a}$$

and

$$\Phi_2(\bar{x},\eta)=\sum_{m=0}^{\infty}B_m\Psi_m(\eta)e^{-\lambda_m\bar{x}} \text{ when } \bar{x}>0. \tag{32b}$$

These axial eigenvalues, β_m and λ_m, for insertion into Eqs. (32a,b) must be positive in order to satisfy the conditions when $\bar{x}\to-\infty$ and $\bar{x}\to+\infty$, respectively. The eigenfunctions in these two equations are selected for a moving plate as

$$\Psi_m(\eta)=\cos(\gamma_m\eta) \tag{33a}$$

with $\eta=y$ and for a moving circular cylinder as Bessel function

$$\Psi_m(\eta)=J_0(\gamma_m\eta) \tag{33b}$$

with $\eta=r$. The eigenvalues are $\gamma_m=m\pi$ for a moving plate and for a moving circular cylinder they are the roots of $J_1(\gamma_m)=0$ with $m=0,1,2,3,\ldots$, for both $\Phi_1(\bar{x},\eta)$ and $\Phi_2(\bar{x},\eta)$ functions. When $m=0$, $\gamma_0=0$ for both passages. Once γ_m is known, both β_m or λ_m is to be determined by inserting $\Phi_1(\bar{x},\eta)$ or $\Phi_2(\bar{x},\eta)$ from Eqs. (32a) or (32b) into Eqs. (31a) or (31b), respectively. Each member of $\Phi_1(\bar{x},\eta)$ function must satisfy Eq. (31a) and each member of $\Phi_2(\bar{x},\eta)$ function must satisfy Eq. (31b). Then, the substitution of $\Phi_1(\bar{x},\eta)$ into Eq. (31a) yields

$$\beta_m=\frac{1}{2}\mathrm{Pe}^2\left[\sqrt{1+4\gamma_m^2/\mathrm{Pe}^2}+1\right] \tag{34a}$$

and the substitution of $\Phi_2(\bar{x},\eta)$ into Eq. (31b) provides

$$\lambda_m=\frac{1}{2}\mathrm{Pe}^2\left[\sqrt{1+4\gamma_m^2/\mathrm{Pe}^2}-1\right]. \tag{34b}$$

Next, the compatibility conditions at $x=0$ are used for the determination of A_m and B_m coefficients. Since $T(0-,\eta)=T(0+,\eta)$, Eqs. (30a,b) produce the relation

$$\Phi_1(0\eta)=\Phi_2(0\eta)+\frac{1}{2}\eta^2. \tag{35a}$$

The use of the second compatibility condition $[\partial T(\bar{x},\eta)/\partial\bar{x}]_{\bar{x}=0-}=[\partial T(\bar{x},\eta)/\partial\bar{x}]_{\bar{x}=0+}$ results in the relation

$$\left[\frac{\partial\Phi_1(\bar{x},\eta)}{\partial\bar{x}}\right]_{\bar{x}=0}=\left[\frac{\partial\Phi_2(\bar{x},\eta)}{\partial\bar{x}}\right]_{\bar{x}=0}+(e+1). \tag{35b}$$

Now, the final solutions for these fluid passages are known after determination of the coefficients A_m and B_m. These solutions have different forms and they are presented separately.

For a moving flat plate, the function $\Psi_m(\eta)$ in (32a,b) becomes $\cos(\gamma_m y)$ with $\gamma_m=m\pi$. Then, by placing $\Phi_1(\bar{x},\eta)$ and $\Phi_2(\bar{x},\eta)$ in the compatibility conditions followed by the application of the orthogonality condition, results in two simultaneous equations

$$A_m-B_m=\frac{1}{N_m}\int_0^1\frac{1}{2}y^2\cos(\gamma_m y)dy=\begin{cases}\frac{1}{6} \text{ when } m=0\\ \frac{2(-1)^m}{\gamma_m^2} \text{ when } m>0\end{cases} \tag{36a}$$

and

$$\beta_mA_m+\lambda_mB_m=\frac{1}{N_m}\int_0^1\cos(\gamma_m y)dy=\begin{cases}1 \text{ when } m=0\\ 0 \text{ when } m>0\end{cases} \tag{36b}$$

where N_m is the norm and $N_m=1$ when $m=0$ while $N_m=1/2$ when $m>0$. For $m=0$, one gets $A_0-B_0=1/6$ from Eq. (36a) and Eqs. (34a,b) provide $\beta_0=\mathrm{Pe}^2$ and $\lambda_0=0$; then, using Eq. (36b) to get $A_0=1/\mathrm{Pe}^2$ and this makes $B_0=1/\mathrm{Pe}^2-1/6$. When $m>0$, the other coefficients are determined from the two Eqs. (36a,b) as

$$A_m=\frac{2(-1)^m}{\gamma_m^2}\frac{\lambda_m}{\lambda_m+\beta_m} \tag{37a}$$

and

$$B_m=-\frac{2(-1)^m}{\gamma_m^2}\frac{\beta_m}{\lambda_m+\beta_m} \tag{37b}$$

while the values of parameters β_m and λ_m are given by Eqs. (34a,b). Finally, the dimensionless temperature becomes

$$\frac{k(T-T_i)}{q_wH}=\frac{1}{\mathrm{Pe}^2}\exp(\mathrm{Pe}^2\bar{x})+\sum_{m=1}^{\infty}\frac{2(-1)^m}{\gamma_m^2}\frac{\lambda_m}{\lambda_m+\beta_m}\cos(\gamma_m y)\times\exp(\beta_m\bar{x}) \tag{38a}$$

when $\bar{x}<0$ and

$$\frac{k(T-T_i)}{q_wH}=\frac{1}{\mathrm{Pe}^2}-\frac{1}{6}+\bar{x}+\frac{1}{2}y^2-\sum_{m=1}^{\infty}\frac{2(-1)^m}{\gamma_m^2}\frac{\beta_m}{\lambda_m+\beta_m}\times\cos(\gamma_m y)\exp(-\lambda_m\bar{x}) \tag{38b}$$

when $\bar{x}\geqslant 0$.

The aforementioned procedure is repeated for a moving circular cylinder for determination of the coefficients A_m and B_m; it results in the following relations:

$$A_m-B_m=\frac{1}{N_m}\int_0^1\frac{1}{2}r^2J_0(\gamma_m r)rdr=\begin{cases}\frac{1}{4} \text{ when } m=0\\ \frac{2}{\gamma_m^2J_0(\gamma_m)} \text{ when } m>0\end{cases} \tag{39a}$$

$$\beta_mA_m+\lambda_mB_m=\frac{2}{N_m}\int_0^1J_0(\gamma_m r)rdr=\begin{cases}2 \text{ when } m=0\\ 0 \text{ when } m>0\end{cases}. \tag{39b}$$

As in the previous case, Eqs. (34a,b) provide $\beta_0=\mathrm{Pe}^2$ and $\lambda_0=0$; this makes $A_0=2/\mathrm{Pe}^2$ and $B_0=2/\mathrm{Pe}^2-1/4$. Furthermore, the other coefficients are obtained as

$$A_m=\frac{2}{\gamma_m^2J_0(\gamma_m)}\frac{\lambda_m}{\lambda_m+\beta_m} \tag{40a}$$

and

$$B_m=\frac{2}{\gamma_m^2J_0(\gamma_m)}\frac{\beta_m}{\lambda_m+\beta_m}. \tag{40b}$$

After appropriate substitutions, Eqs. (30a,b) would produce the following temperature solutions

$$\frac{k(T-T_i)}{q_wH}=\frac{1}{\mathrm{Pe}^2}\exp(\mathrm{pe}^2\bar{x})+\sum_{m=1}^{\infty}\frac{2}{\gamma_m^2J_0(\gamma_m)}\left(\frac{\lambda_m}{\lambda_m+\beta_m}\right)J_0(\gamma_m r)\times\exp(\beta_m\bar{x}) \tag{41a}$$

when $\bar{x}<0$ and

$$\frac{k(T-T_i)}{q_wH}=\frac{2}{\mathrm{Pe}^2}-\frac{1}{4}+2\bar{x}+\frac{1}{2}r^2-\sum_{m=1}^{\infty}\frac{2}{\gamma_m^2J_0(\gamma_m)}\left(\frac{\beta_m}{\lambda_m+\beta_m}\right)J_0(\gamma_m r)\exp(\lambda_m\bar{x}) \tag{41b}$$

when $\bar{x}\geqslant 0$.

4. Numerical results and discussions

The dash line with circular symbols in Fig. 5 describes the wall temperature for the moving semi-infinite domain from Eq. (22b), also plotted in Fig. 2. The abscissa in Fig. 2 and in Fig. 5 is $x\mathrm{Pe}=U\hat{x}/\alpha$, independent of the characteristic length. Furthermore, Fig. 5 shows the computed values of the dimensionless wall temperature from Eq. (38b), when $\hat{x}>0$, for a moving flat plate using different Peclet numbers $\mathrm{Pe}=UH/\alpha$. This figure indicates that the dimensionless wall temperature reduces as Pe increases, when Pe is relatively small. However, as Pe becomes larger, the lines

converge to the single limiting dash line with circular symbols for the semi-infinite domain. Indeed, this figure shows that the data in Fig. 2 serve as a limiting solution as Pe increases beyond 5. This phenomenon is expected as discussed in an earlier section. Additionally, for slug flow between two parallel plates, Fig. 6 shows the corresponding computed Stanton number values

$$\mathrm{St} = \frac{q_w}{\rho c_p U(T_w - T_i)} \tag{42}$$

at different Peclet. As expected from an earlier discussion, when Pe increases to beyond 5, the plotted St values approach their limiting values as they appear in Fig. 3.

Therefore, the Stanton number for a moving semi-infinite medium serves as an upper limit for a moving plate or for a slug flow between two parallel plates. The aforementioned formulations show that this upper limit behavior should hold for other passages. To demonstrate this issue, the Stanton number is numerically determined for slug flow in a circular duct from Eq. (41b). Fig. 7 indicates that the computed values of the Stanton number show similar behaviors as those presented in Fig. 6.

It was noted that Eqs. (38a,b) and (41a,b) are well-behaved series solutions with rapid convergence when Pe < 1. Indeed for Pe ⩽ 0.5, a solution with a single eigenvalue can produce a relatively accurate solution over the entire range of $U\hat{x}/\alpha$ parameter. For Pe > 1, a moderate increase in the number of eigenvalues is adequate until Pe becomes very large. Of course at large values of Pe, the solution given by Eq. (22b) yields an asymptotic solution at small $U\hat{x}/\alpha$ parameter, as shown in Fig. 6 for Pe > 5 and in Fig. 7 for Pe > 10. Also, as an illustration for small $2(\omega x) = U\hat{x}/\alpha$, Eq. (22b) with asymptotic values from Eqs. (24a,b) takes a simpler form

$$\frac{\rho c_p U\theta(x,0)}{q_w} = \frac{e^{\omega x}}{\pi}\left\{2 - 0.5772(\omega x)[2 + (\omega x)^2] - (\omega x)[2 - (\omega x) + (\omega x)^2]\ln(\omega x)\right\} \tag{43}$$

with an error of less than 1% for $U\hat{x}/\alpha \leqslant 1$.

The determination of the commonly used heat transfer coefficient $h = q_w/(T_w - T_b)$ is the next subject of this presentation. The method of determination of the wall temperature is in the earlier presentation. For slug flow between two parallel plates, the bulk temperature values are obtained from the relations

$$T_{b,1} - T_i = \frac{1}{H}\int_0^H (T_1 - T_i)d\hat{y} = \left(\frac{q_w H}{k}\right)\frac{\exp\left(-\mathrm{Pe}^2|\bar{x}|\right)}{\mathrm{Pe}^2} \tag{44a}$$

when $\bar{x} < 0$ and

$$T_{b,2} - T_i = \frac{1}{H}\int_0^H (T_2 - T_i)d\hat{y} = \left(\frac{q_w H}{k}\right)\left(\frac{1}{\mathrm{Pe}^2} + \bar{x}\right) \tag{44b}$$

when $\bar{x} > 0$. Also, for slug flow through a circular duct, the bulk temperature can be determined using the relations

$$T_{b,1} - T_i = \frac{1}{\pi r_0^2}\int_0^{r_0} (T_1 - T_i)2\pi\hat{r}d\hat{r} = \left(\frac{q_w r_0}{k}\right)\frac{2\exp\left(-\mathrm{Pe}^2|\bar{x}|\right)}{\mathrm{Pe}^2} \tag{45a}$$

when $\bar{x} < 0$ and

$$T_{b,2} - T_i = \frac{1}{\pi r_0^2}\int_0^{r_0} (T_1 - T_i)2\pi\hat{r}d\hat{r} = \left(\frac{q_w r_0}{k}\right)\left(\frac{2}{\mathrm{Pe}^2} + 2\bar{x}\right) \tag{45b}$$

when $\bar{x} > 0$. It is to be noted from Eqs. (44a), (45a) that, when $\bar{x} = 0$, the dimensionless bulk temperature becomes $[T_{b,1}(0) - T_i]/(q_w H/k) = 1/\mathrm{Pe}^2$ for parallel-plate ducts and it is equal to $2/\mathrm{Pe}^2$ for circular ducts. Also, a comparison of Eq. (44b) with Eq. (45b) indicates that the bulk temperature in Eq. (45b) increases at a higher rate than bulk temperature in Eq. (44b) as $\bar{x}$ increases. Furthermore, the wall temperatures from Eq. (41b) exhibit similar behaviors and increases faster than the wall temperature from Eq. (38b), as $\bar{x}$ increases.

Since the wall temperature and the bulk temperature are readily available, it is possible to determine the Nusselt number $\mathrm{Nu}_D = hD_h/k$ parallel plate passage where $D_h = 4H$ is the hydraulic diameter and $h = q_w/(T_w - T_b)$. The computed Nusselt number values plotted in Fig. 8 show the variation of

$$\mathrm{Nu}_D = \frac{4q_w H}{k(T_w - T_b)} \tag{46a}$$

as a function of $\bar{x}$ for different Peclet numbers. As can be seen from Fig. 8, the Nusselt number has a finite value as $\bar{x}$ goes toward zero

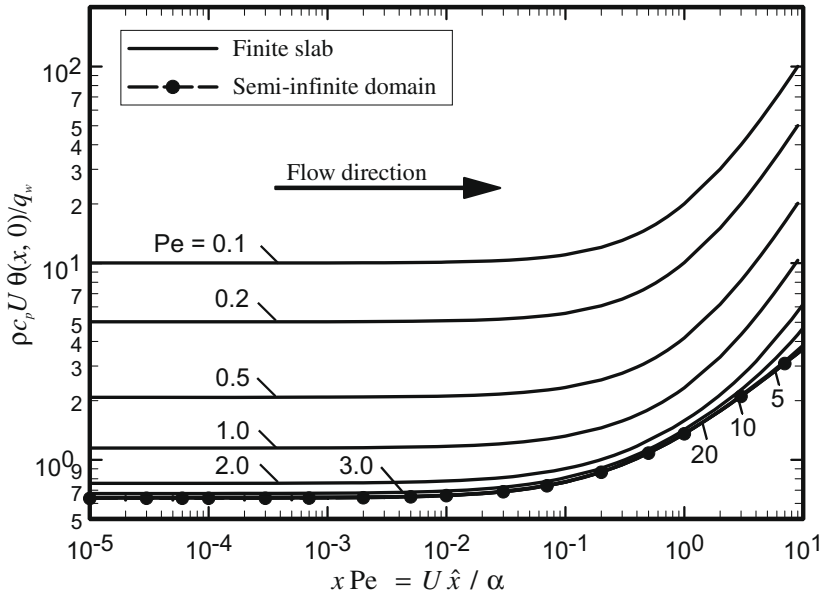

Fig. 5. A comparison of the wall temperature for parallel plate channels with those from a semi-infinite flow field.

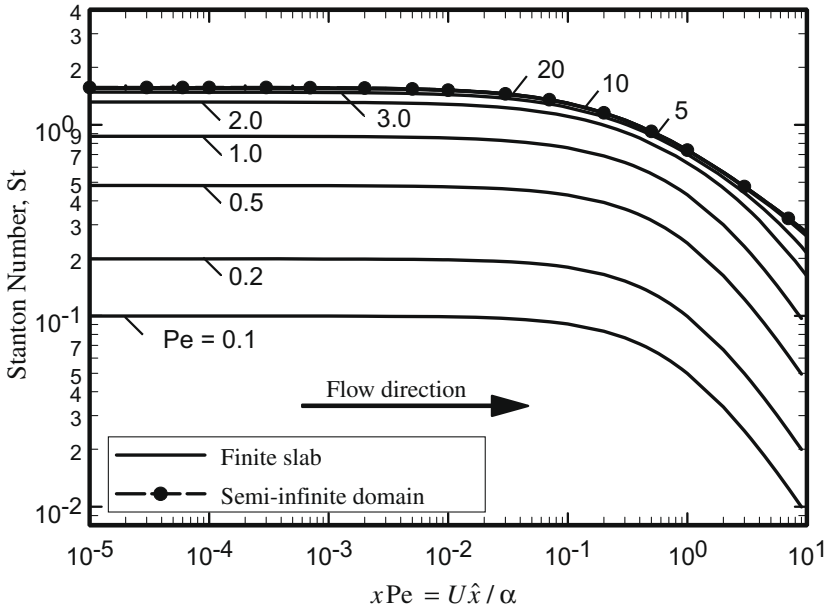

Fig. 6. A comparison of the computed Stanton numbers for slug flow in parallel-plate ducts with those for a semi-infinite medium.

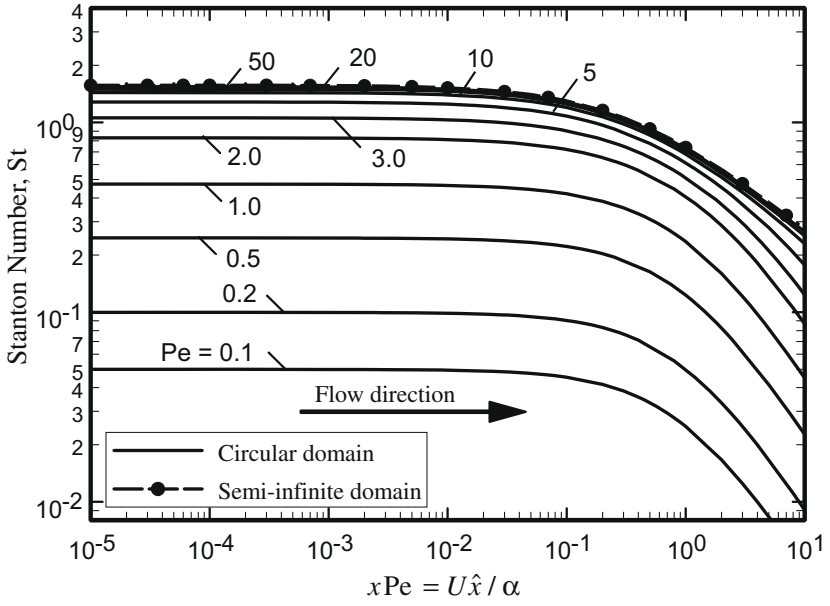

Fig. 7. A comparison of the computed Stanton numbers for slug flow in circular ducts with those for a semi-infinite medium.

and it approaches $\mathrm{Nu}_D = 12$ as $\bar{x}$ becomes very large. Also, for circular passages with $D_h = 4r_0$, the calculated Nusselt number

$$\mathrm{Nu}_D = \frac{2q_w r_0}{k(T_w - T_b)} \tag{46b}$$

values for this passage are plotted in Fig. 9. The plotted lines in Fig. 9 show similar behaviors as those in Fig. 8 when $\bar{x}$ is relatively small. However, the lines in Fig. 8 have smaller values than those in Fig. 8 for the same Peclet numbers while they all approach an asymptotic value of 8 as $\bar{x}$ becomes very large.

The information from the slug flow within these passages with prescribed wall heat flux can become a useful tool for the study of heat transfer in porous passages. It can provide limiting solutions for these passages, as the porosity reduces. As an application to classical conduction in moving solid bodies, these limiting solutions become valuable when a moving wall is heated discretely. Because the working partial differential equation and boundary conditions are linear, one can use superposition of two solutions. As an example, for a single heat source between $x = 0$ and $x = x_1$, the temperature field becomes

$$\Delta\theta(x,y) = \theta(x,y) - \theta(x - x_1, y). \tag{47}$$

This methodology can be extended when there are multiple heating sites. It is to be noted that each θ solution contains the contributions from positive and negative sides of its axial coordinate.

5. Conclusion

The computed information show that the Stanton number has a maximum value of $\pi/2$ at $x = 0$ where a step change in temperature

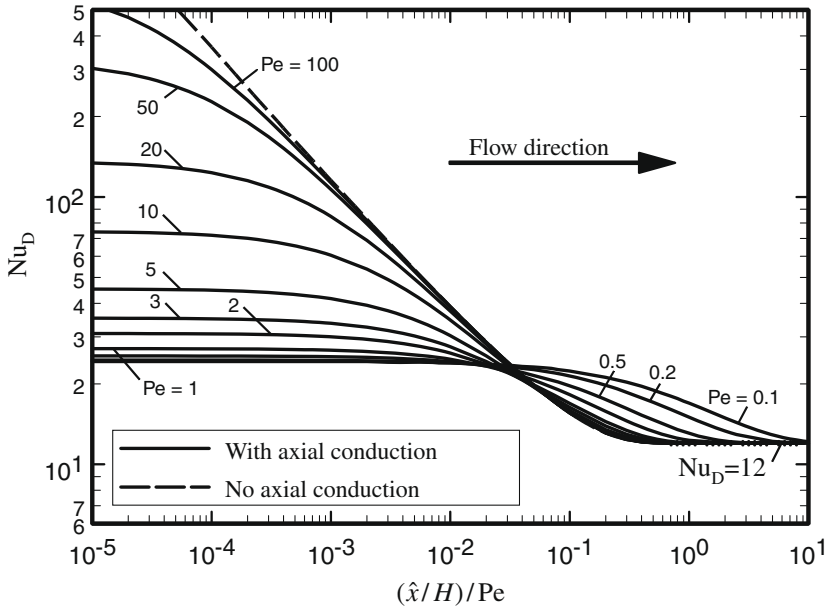

Fig. 8. The Nusselt number for slug flow between two parallel plates with a step change in the wall heat flux.

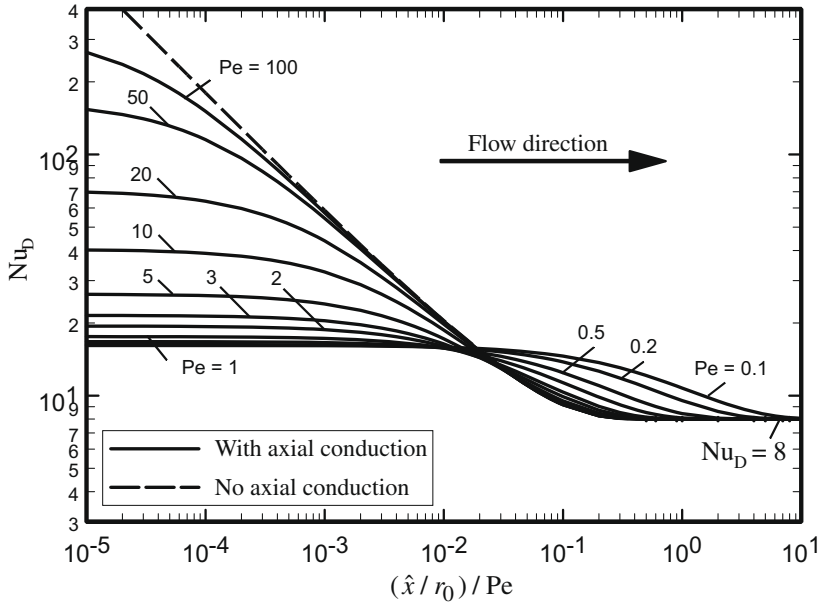

Fig. 9. The Nusselt number for slug flow within circular passages with a step change in the wall heat flux.

occurs and it gradually reduces as x increases. The presence of another wall also contributes to the axial conduction in the neighborhood of the thermal entrance location. This phenomenon causes increase in the temperature of the approaching fluid from $x \leqslant 0$ location in the thermal entrance regions of parallel-plate ducts, circular pipes, and those with two-dimensional cross sections, e.g., in rectangular and triangular ducts. Additionally, since the Stanton number for slug flow is larger than that for flow with other velocity profiles, it serves as an upper limit.

Furthermore, available studies show that neglecting axial conduction produces an infinite heat transfer coefficient at the location where a step change in the surface heat flux occurs. Since a value of $St = \pi/2$ serves as an upper limit and is far less than infinity, the axial conduction in ducts should not be ignored unless the Peclet number is relatively large, as shown in Figs. 8 and 9.

References

[1] H.C. Agrawal, Heat transfer in laminar flow between parallel plates at small Peclet numbers, Appl. Sci. Res. A 9 (1) (1960) 177–189.
[2] D.K. Hennecke, Heat transfer by Hagen-Poiseuille flow in the thermal development region with axial conduction, Warme Stoffubertrag. 1 (3) (1968) 177–184.
[3] Y. Bayazitoglu, N.M. Ozisik, On the solution of Graetz type problem with axial conduction, Int. J. Heat Mass Transfer 23 (10) (1981) 1399–1402.
[4] C.A. Deavours, An exact solution of temperature distribution in parallel plate Poiseuille flow, J. Heat Transfer 96 (4) (1974) 489–495.
[5] M.L. Michelsen, J. Villadsen, The Graetz problem with axial heat conduction, Int. J. Heat Mass Transfer 17 (11) (1974) 1391–1402.
[6] C.E. Smith, M. Faghri, On the determination of temperature distribution in laminar pipe flow with a step change in wall heat flux, J. Heat Transfer 97 (1) (1975) 137–139.
[7] A. Campo, J.C. Auguste, Axial conduction in laminar pipe flows with nonlinear wall heat flux, Int. J. Heat Mass Transfer 21 (12) (1978) 1597–1607.

[8] B.M. Vick, N.M. Ozisik, Y. Bayazitoglu, A method of analysis of low Peclet number thermal region problems with axial conduction, Lett. Heat Mass Transfer 7 (4) (1980) 235–248.
[9] E. Papoutsakis, D. Ramkrishna, The extended Graetz problem with prescribed wall heat flux, AIChE J. 26 (5) (1980) 779–787.
[10] B.M. Vick, N.M. Ozisik, An exact analysis of low Peclet number heat transfer in laminar flow axial conduction, Lett. Heat Mass Transfer 8 (1) (1981) 1–10.
[11] A.S. Telles, E.M. Queiroz, G.E. Filho, Solutions of the extended Graetz problem, Int. J. Heat Mass Transfer 44 (2) (2001) 471–483.
[12] J. Lahjomri, A. Oubarra, Analytical solution of the Graetz problem with axial conduction, J. Heat Transfer 121 (4) (1999) 1078–1083.
[13] I. Tiselj, G. Hetsroni, B. Mavko, A. Mosyak, E. Pogrebnyak, Z. Segal, Effect of axial conduction on the heat transfer in micro-channels, Int. J. Heat Mass Transfer 47 (12–13) (2004) 2551–2565.
[14] A. Haji-Sheikh, D.E. Amos, J.V. Beck, Axial heat conduction of heat through a moving fluid in a semi-infinite region, Int. J. Heat Mass Transfer 51 (19–20) (2008) 4651–4658.
[15] A. Haji-Sheikh, J.V. Beck, D.E. Amos, Axial heat conduction effects in the entrance region of parallel plate ducts, Int. J. Heat Mass Transfer 51 (25–26) (2008) 5811–5822.
[16] A. Haji-Sheikh, J.V. Beck, D.E. Amos, Axial heat conduction effects in the entrance region of circular ducts, Heat Mass Transfer J 45 (3) (2009) 331–341.
[17] D.A. Nield, A. Bejan, Convection in Porous Media, third ed., Springer-Verlag, New York, 2006.
[18] D.A. Nield, A.V. Kuznetsov, M. Xiong, Thermally developing forced convection in a porous medium: parallel plate channel with walls at uniform temperature, with axial conduction and viscous dissipation effects, Int. J. Heat Mass Transfer 46 (4) (2003) 643–651.
[19] D.A. Nield, A.V. Kuznetsov, M. Xiong, Thermally developing forced convection in a porous medium: circular ducts with walls at constant temperature, with longitudinal conduction and viscous dissipation effects, Trans. Porous Med. 53 (3) (2003) 331–345.
[20] W.J. Minkowycz, A. Haji-Sheikh, Heat transfer in parallel plates and circular porous passages with axial conduction, Int. J. Heat Mass Transfer 49 (13–14) (2006) 2381–2390.
[21] A. Erdelyi, W. Magnus, F. Oberhettinger, F.G. Tricomi, Tables of Integral Transforms, vol. 1, McGraw-Hill, New York, 1954.
[22] I.S. Gradshteyn, I.M. Ryzhik, Table of integrals, series, and products, in: Alan Jeffrey (Ed.), fifth ed., Academic Press Inc., 1994.
[23] M. Abramowitz, I.A. Stegun, Handbook of Mathematical Functions, National Bureau of Standards Applied Mathematics Series 55, 1965.